

Prospects for measuring $|V_{ts}|$ at the LHC.

F. Barreiro^{*†}

Universidad Autonoma de Madrid

E-mail: fernando.barreiro@uam.es

We study the prospects of measuring the CKM matrix element $|V_{ts}|$ at the LHC with the top quarks produced in the processes $pp \rightarrow t\bar{t}X$ and $pp \rightarrow t/\bar{t}X$, and the subsequent decays $t \rightarrow W^+s$ and $\bar{t} \rightarrow W^-\bar{s}$. To reduce the jet activity in top quark decays, we insist on tagging the W^\pm leptonically, $W^\pm \rightarrow \ell^\pm \nu_\ell$ ($\ell = e, \mu, \tau$), and analyse the anticipated jet profiles in the signal process $t \rightarrow Ws$ and the dominant background from the decay $t \rightarrow Wb$. To that end, we analyse the $V0$ (K^0 and Λ) distributions in the s - and b -quark jets concentrating on the energy and transverse momentum distributions of these particles. Noting that the $V0$ s emanating from the $t \rightarrow Wb$ branch have displaced decay vertexes from the interaction point due to the weak decays $b \rightarrow c \rightarrow s$, and that the b -quark jets are rich in charged leptons, the information from the secondary vertex distributions and the absence of energetic charged leptons in the jet provide additional (b -jet vs. s -jet) discrimination in top quark decays. These distributions are used to train a boosted decision tree (BDT), a technique used successfully in measuring the CKM matrix element $|V_{tb}|$ in single top production at the Tevatron. We show that the BDT-response functions corresponding to the signal ($t \rightarrow Ws$) and background ($t \rightarrow Wb$) are very different. Detailed simulations undertaken by us with the Monte Carlo generator PYTHIA are used to estimate the background rejection versus signal efficiency for two representative LHC energies $\sqrt{s} = 7$ TeV and 14 TeV. We argue that a benchmark with 5% signal ($t \rightarrow Ws$) efficiency and a background ($t \rightarrow bW$) rejection by a factor 10^3 (required due to the anticipated value of the ratio $|V_{ts}|^2/|V_{tb}|^2 \simeq 1.6 \times 10^{-3}$) can be achieved at the LHC, given the promised luminosity.

*36th International Conference on High Energy Physics,
July 4-11, 2012
Melbourne, Australia*

^{*}Speaker.

[†]This work, done in collaboration with A. Ali and Th. Lagouri, is supported by MICINN under contract FPA-2008-0601.

1. Introduction

It is now fifteen years that the top quark was discovered in proton-antiproton collisions at the Tevatron [1]. Since then, a lot of precise measurements have been undertaken at Fermilab and more recently at the LHC. Among the highlights are the measurements of the top quark mass, limited at present by a systematic uncertainty of about 1.0%, [2], the $t\bar{t}$ production cross section with about 7% accuracy [3], and the measurement of the electroweak single top production [4]. Of these, the single top (or anti-top) production cross section depends on the charged current couplings tqW , where $q = d, s, b$, which in the standard model (SM) are governed by the Cabibbo-Kobayashi-Maskawa (CKM) quark mixing matrix V_{CKM} [5, 6], which in the Wolfenstein [7] parametrization is expressed as

$$V_{CKM} \equiv \begin{pmatrix} V_{ud} & V_{us} & V_{ub} \\ V_{cd} & V_{cs} & V_{cb} \\ V_{td} & V_{ts} & V_{tb} \end{pmatrix} \simeq \begin{pmatrix} 1 - \frac{1}{2}\lambda^2 & \lambda & A\lambda^3(\rho - i\eta) \\ -\lambda(1 + iA^2\lambda^4\eta) & 1 - \frac{1}{2}\lambda^2 & A\lambda^2 \\ A\lambda^3(1 - \rho - i\eta) & -A\lambda^2(1 + i\lambda^2\eta) & 1 \end{pmatrix}$$

The cross section $\sigma(p\bar{p} \rightarrow t/\bar{t}X)$ has provided a direct measurement of the dominant CKM-matrix element $|V_{tb}|$. The ATLAS measurements yield $|V_{tb}| = 1.13 \pm 0.14(\text{stat}) \pm 0.11(\text{sys})$, which in turn gives $|V_{tb}| > 0.75$ at 95% C.L. [4] and similar number for CMS.

The above determination of the matrix element $|V_{tb}|$, can be compared with the indirect determination based on a number of loop-induced processes in which top quark participates as a virtual state, such as the B^0 - \bar{B}^0 and B_s^0 - \bar{B}_s^0 mixings, the radiative decay $B \rightarrow X_s\gamma$ and the CP-violation parameter ε_K in the Kaon sector. Overall fits of the CKM unitarity yield, comparatively speaking, an infinitely more accurate value $|V_{tb}| = 0.999133(44)$ [8]. Experiments at the LHC are expected to reach an accuracy of $O(1)\%$ on $|V_{tb}|$, which will provide valuable constraints on a number of extensions of the standard model.

Encouraged by these measurements, we go a step further and explore in this paper the prospects of measuring the matrix element $|V_{ts}|$ at the LHC. Unitarity fits yield $|V_{ts}| = 0.0407 \pm 0.001$ [8] and $|V_{td}| = (8.74_{-0.37}^{+0.26}) \times 10^{-3}$. Direct determination of these matrix elements will require a good tagging of the $t \rightarrow s$ transition (for $|V_{ts}|$) and $t \rightarrow d$ transition (for $|V_{td}|$) in the top quark decays. Lacking a good tagging for the $t \rightarrow d$ transition, and also because of the small size of the CKM-matrix element, we concentrate here on the measurements of $|V_{ts}|$ at the LHC.

In order to measure $|V_{ts}|$ directly, one has to develop efficient tagging of the decay $t \rightarrow W s$ and suppress the dominant decay $t \rightarrow W b$. As the first step, we propose to tag only those events in which the W^\pm decay leptonically to reduce the jet activity in top quark decays. We suggest tagging the leading particle in the emerging s-quark jet, expected to be a $V0$ (K^0 and Λ), and study their energy and transverse momentum distributions. Energetic $V0$ s are also present in the b -quark jets initiated by the decay $t \rightarrow W b$ and the subsequent weak decays $b \rightarrow c \rightarrow s$. However, in this case, the $V0$ s will have displaced vertexes (from the interaction point) and they will be often accompanied with energetic charged leptons due to the decays $b \rightarrow \ell^\pm X$. Absence of a secondary vertex and paucity of the energetic charged leptons in the jet provide a strong discrimination on the decays $t \rightarrow Wb$ without compromising the decays $t \rightarrow Ws$. The secondary decay vertex distributions in the variable called r in the figures are of principal interest. Here r is the distance traversed in the transverse plane by the b -quark before decaying, which is smeared with a Gaussian resolution to

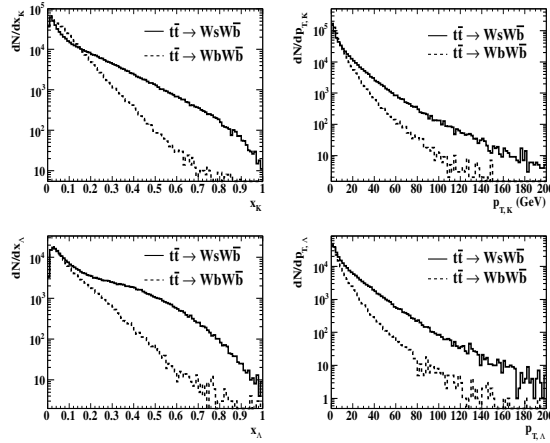


Figure 1: $pp \rightarrow t\bar{t}X$ at $\sqrt{s} = 14$ TeV. Upper left frame: scaled- K^0 -energy distributions dN/dx_K from $t \rightarrow W s(\rightarrow K^0X)$ (upper histogram) and $t \rightarrow W b(\rightarrow K^0X)$ (lower histogram). Upper right frame: Transverse momentum distributions of the K^0 s measured w.r.t. beam axis $dN/dp_{T,K}$ (in GeV) in the same production and decay processes as in the left frame. Lower frames show the distributions dN/dx_{Λ} and $dN/dp_{T,\Lambda}$ (in GeV) for $t \rightarrow W s(\rightarrow \Lambda X)$ (upper histogram) and $t \rightarrow W b(\rightarrow \Lambda X)$ (lower histogram).

take into account realistic experimental conditions. We have assumed two representative r.m.s. values (1 mm and 2 mm) for the Gaussian, where probably 2 mm is more realistic.

Having generated these distributions, characterising the signal $t \rightarrow Ws$ and background $t \rightarrow Wb$ events, we use a technique called the Boosted Decision Trees (BDT) to develop an ID optimised for the $t \rightarrow Ws$ decays. BDT, or a variant of it called BDTD, where (De)correlated variables are used, is a powerful tool in discriminating signal events from large backgrounds. We have provided the detailed profile of the various kinematic variables for the signal ($t \rightarrow Ws$) and the background ($t \rightarrow Wb$) on an event-by-event basis with the help of the Monte Carlo generator. The software called the Toolkit for Multivariate Data Analysis in ROOT (TMVA) [9] is used for the BDT response in our analysis. We argue that a benchmark with 5% signal ($t \rightarrow Ws$) efficiency and a background ($t \rightarrow Wb$) rejection by a factor 10^3 can be achieved at the LHC, given the projected LHC luminosity. We note that this level of background rejection is required due to the anticipated value of the ratio $|V_{ts}|^2/|V_{tb}|^2 \simeq 1.6 \times 10^{-3}$.

2. Analysis of the process $pp \rightarrow t\bar{t}X$ and the subsequent decays $t \rightarrow Wb, Ws$

Theoretical predictions of the top quark production at the LHC have been obtained by including up to the next-to-next-to-leading order (NNLO) corrections in the strong coupling constant.

A typical estimate is: $\sigma(pp \rightarrow t\bar{t}X) = 874_{-33}^{+14}$ pb for $m_t = 173$ GeV and $\sqrt{s} = 14$ TeV, where the errors reflect the combined uncertainties in the factorisation and normalisation scales and in the parton distribution functions (PDF). Thus, using an integrated luminosity of 10 fb^{-1} per year as a benchmark, one expects an annual yield of $O(10^7)$ $t\bar{t}$ events at the LHC@14 TeV. The cross sections at the lower LHC energies, 7 and 10 TeV, have also been calculated, with $\sigma(pp \rightarrow t\bar{t}X) \simeq 400$ pb

at 10 TeV and about half that number at 7 TeV. Thus, for the top quark physics, the dividends in going from 7 to 14 TeV are higher by a good factor 4.

For the numerical results shown here we have used the PYTHIA Monte Carlo [11] to generate 10^6 events for the process $pp \rightarrow t\bar{t}X$, followed by the decay chains $t \rightarrow W^+b$, W^+s and $\bar{t} \rightarrow W^-\bar{b}$, $W^-\bar{s}$. As stated in the introduction, the W^\pm are forced to decay only leptonically $W^\pm \rightarrow \ell^\pm \nu_\ell$ ($\ell = e, \mu, \tau$) to reduce the jet activity from the non-leptonic decays of the W^\pm . This corresponds to an integrated luminosity of 10 fb^{-1} at 14 TeV. For an estimated efficiency of 5% at a background rejection of 10^{-3} and $|V_{ts}|^2 \sim 1.7 \times 10^{-3}$, we expect $0.05 \times 2 \times 1.7 \times 10^{-3} \times 10^6 = 170$ events over a background of $10^{-3} \times 10^6 = 10^3$ events giving a significance of $170/\sqrt{1000}$ i.e. more than 5σ .

We then concentrate on the $V0$ production, which for the experimental conditions at the two main detectors ATLAS and the CMS implies $V0 = K_S^0$ or $V0 = \Lambda$, as the long-lived K_L^0 will decay mostly out of the detectors. However, both K_S^0 and Λ^0 can be detected by ATLAS and CMS and their energy and momentum measured with reasonably good precision. In the present analysis, we reconstruct $V0$'s and soft leptons in the rapidity range $|\eta| \leq 2.5$. In addition, we require the $V0$'s decay radius to lie in the range 20 to 600 mm. These acceptance cuts are acceptable for both multipurpose detectors mentioned above, and they will be used in the analysis described in this and the next section.

We start by showing the distributions for $\sqrt{s} = 14$ TeV, the designed LHC center-of-mass energy. The energy distribution of the K_S^0 is shown in the left-hand frame in Fig 1 plotted as a function of the scaled energy of the Kaons $X_K = E_K/E_{\text{jet}}$. The transverse momentum of the K^0 s, $p_T(K^0)$ (in GeV) is shown in the right hand frame in Fig 1. In both of these frames, the upper histograms correspond to the decay $t \rightarrow Ws$ and the lower one to the decay $t \rightarrow Wb$. As expected, the decay chain $t \rightarrow Ws(\rightarrow K_S^0)$ has a much stiffer distribution both in X_K and $p_T(K^0)$, as the K^0 's descending from the decay chain $t \rightarrow Wb(\rightarrow c \rightarrow s)$ are rapidly degraded in these variables due to the subsequent weak decays. The corresponding distributions for the Λ s are shown in the lower two frames in Fig. 1. They are qualitatively very similar to those of the K^0 s.

We now show the distributions in the charged lepton energy from the decays $t \rightarrow b \rightarrow \ell^\pm X$ and $t \rightarrow s \rightarrow \ell^\pm X$ in Fig. 2, showing the scaled lepton energy in the variable $X_\ell = E_\ell/E_{\text{jet}}$ (upper left frame) and in p_T^ℓ , the transverse momentum of the charged leptons (upper right frame). This distribution quantifies the richness of the b -jets in charged leptons and the stiff character of the energy/transverse momentum distributions due to the weak decays, as compared to the leptons from $s \rightarrow \ell^\pm X$, which are all soft and coming from the leptonic decays of the various resonances produced in the fragmentation of the s -quark. The final set of distributions from our Monte Carlo simulation is the secondary decay vertex distribution (lower frame), smeared with a Gaussian distribution with a r.m.s. of 2 millimetres, shown in terms of a variable called r (measured in millimetres). The decay length for the $t \rightarrow Wb$ case is calculated as $\gamma c\tau_b$, where γ is the Lorentz factor, and $c\tau_b = 0.45$ mm, corresponding to an average b -quark lifetime taken as $\tau_b = 1.5$ ps from the PDG [8]. This distribution, which reflects the long lifetime of the b -quark (respectively of the B and Λ_b hadrons), against the lack of any secondary vertex from the s -quark fragmentation process, is also a very powerful discriminant of $t \rightarrow Wb$ vs. $t \rightarrow Ws$ decays.

Having generated these distributions, characterising the signal $t \rightarrow Ws$ and background $t \rightarrow Wb$ events in the process $pp \rightarrow t\bar{t}X$ at the LHC, we use the BDT technique, discussed in the

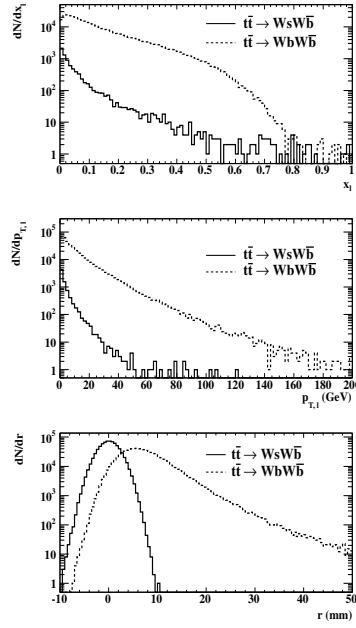


Figure 2: $pp \rightarrow t\bar{t}X$ at $\sqrt{s} = 14$ TeV. Upper frame: scaled- ℓ^\pm -energy distributions, dN/dx_ℓ , from $t \rightarrow Ws$ ($\rightarrow \ell^\pm X$) (lower histogram) and $t \rightarrow Wb$ ($\rightarrow \ell^\pm X$) (upper histogram). Middle frame: Transverse momentum distributions of the ℓ^\pm s measured w.r.t. beam axis, $dN/dp_{T\ell}$ (in GeV), in the same production and decay processes as in the upper frame. Lower frame: Secondary decay vertex distributions in the variable r (in millimetres) for the two decay chains $t \rightarrow Ws$ (solid histogram) and $t \rightarrow Wb$ (dashed histogram), obtained by smearing the decay length with a Gaussian having an r.m.s. value 2 millimetres.

introduction. In Fig. 3, we show the BDT response functions, showing that a clear separation between the signal ($t \rightarrow Ws$) and background ($t \rightarrow Wb$) events has been achieved. The background rejection vs. signal efficiency for the $pp \rightarrow t\bar{t}$ events is shown in Fig. 3. The results are shown numerically in Table 1.

The distributions at $\sqrt{s} = 7$ and 10 TeV are very similar to the corresponding ones shown in Fig. 1 for 14 TeV. Hence, the characteristic differences that we have shown at $\sqrt{s} = 14$ TeV emanating from the top quark decays $t \rightarrow Wb$ and $t \rightarrow Ws$ in the $V0$ and charged lepton energy- and transverse momentum spectra are also present at the lower energies.

We have calculated the tagging efficiencies for the decay $t \rightarrow Ws$ (signal) for an acceptance of 0.1% for the decay $t \rightarrow Wb$ (background). The acceptance level is motivated by the anticipated value of the ratio of the $t \rightarrow Ws$ and $t \rightarrow Wb$ decay rates, which in the SM is $O(10^{-3})$. The tagging efficiencies for the three centre-of-mass energy at the LHC (7, 10 and 14 TeV) are given in Table 1 for two different vertex smearing (1 mm and 2 mm), assuming a Gaussian distribution.

Results for single top production can be found in [10].

References

- [1] F. Abe *et al.* [CDF Coll.], Phys. Rev. Lett. **74**, 2626 (1995) and S. Abachi *et al.* [D0 Coll.], Phys. Rev. Lett. **74**, 2632 (1995).

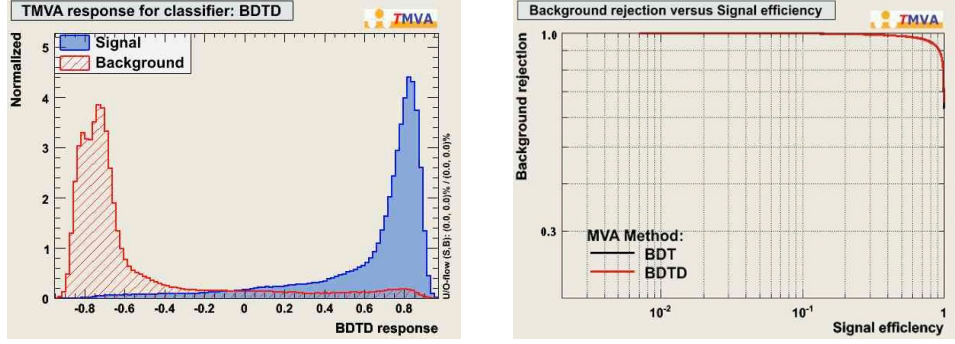


Figure 3: $pp \rightarrow t\bar{t}X$ at $\sqrt{s} = 14$ TeV. Left: The normalised BDTD response. The signal (dark shaded) from the decay $t \rightarrow Ws$ and the background (light shaded) from the decay $t \rightarrow Wb$ are clearly separated in this variable. Right: Background rejection vs. signal efficiency from the previous BDTD response. The two MVA methods yield very similar results.

Table 1: Tagging efficiencies (in %) for the process $pp \rightarrow t\bar{t}X$, followed by the decay $t \rightarrow Ws$ (signal) and $t \rightarrow Wb$ (background), calculated for an acceptance of 0.1% for the background at three LHC centre-of-mass energies. Two Gaussian vertex smearing (with r.m.s. values 2 mm and 1 mm) are assumed for calculating the displaced vertex distributions dN/dr .

σ_0	7 TeV	10 TeV	14 TeV
2 mm	5.1	5.6	5.0
1 mm	20.5	15.4	15.5

- [2] G. Aad *et al.* [ATLAS Coll.], Eur. Phys. Jour. C72 (2012) 2046, and S. Chatrchyan *et al.* [CMS Coll.], Eur. Phys. Jour. C 72 (2012) 2202.
- [3] G. Aad *et al.* [ATLAS Coll.], Phys. Lett. B 711 (2012) 244, and S. Chatrchyan *et al.* [CMS Coll.], Phys. Rev. D 84 (2011) 092004.
- [4] G. Aad *et al.* [ATLAS Coll.], Phys. Lett. B 717 (2012) 330, and S. Chatrchyan *et al.* [CMS Coll.], Phys. Rev. Lett. 107 (2011) 091802.
- [5] N. Cabibbo, Phys. Rev. Lett. **10**, 531 (1963).
- [6] M. Kobayashi and T. Maskawa, Prog. Theor. Phys. **49**, 652 (1973).
- [7] L. Wolfenstein, Phys. Rev. Lett. **51**, 1945 (1983).
- [8] C. Amsler *et al.* [Particle Data Group], Phys. Lett. B **667**, 1 (2008).
- [9] A. Hocker *et al.*, PoS A CAT, 040 (2007) [arXiv:physics/0703039].
- [10] A. Ali, F. Barreiro and Th. Lagouri, Phys. Lett. B **693**, 44 (2010).
- [11] T. Sjostrand, S. Mrenna and P. Z. Skands, Comput. Phys. Commun. **178**, 852 (2008) [arXiv:0710.3820 [hep-ph]].
- [12] N. Kidonakis, Nucl. Phys. A **827**, 448C (2009) [arXiv:0901.2155 [hep-ph]].